ECS Digital Library
JOURNAL OF THE ELECTROCHEMICAL SOCIETY
ELECTROCHEMICAL AND SOLID-STATE LETTERS
ECS TRANSACTIONS
MEETING ABSTRACTS
INTERFACE
HISTORY CENTER
MANUSCRIPT SUBMISSIONS
ECS BOOKSTORE
SUBSCRIPTION INFORMATION
COPYRIGHT REQUESTS
ADVERTISING OPPORTUNITIES
ECS Info
Support the Future
Renew Now

Search All Issues

[Back to Search Query | Start New Search | Searching Hints]

You were searching for : (Organic Thin-Film Transistors with Short) RSS

You found 1 out of 75944 (1 returned) Documents 1 - 1 listed on this page

Options for selected Articles | View MyArticles

Check Article(s) then ... Go

Select up to 20 articles at a time. YOUR CART

38% 1. **Organic Thin-Film Transistors with Short Channel Length Fabricated by Reverse Offset Printing**

Minseok Kim, In-Kyu You, Hyun Han, Soon-Won Jung, Tae-Youb Kim, Byeong-Kwon Ju, and Jae Bon Koo

Electrochem. Solid-State Lett. **14** H333 (2011) Full Text: [HTML PDF (1199 kB)] Order Document

[Back to Search Query | Start New Search | Searching Hints]

Electrochemical and Solid-State Letters, **14** (8) H333-H336 (2011)
1099-0062/2011/14(8)/H333/4/$28.00 © The Electrochemical Society

Organic Thin-Film Transistors with Short Channel Length Fabricated by Reverse Offset Printing

Minseok Kim,[a,b] In-Kyu You,[a] Hyun Han,[a,c] Soon-Won Jung,[a] Tae-Youb Kim,[a] Byeong-Kwon Ju,[b,z] and Jae Bon Koo[a,z]

[a]*Convergence Components and Materials Research Laboratory, Electronics and Telecommunications Research Institute, Yuseong-gu, Daejeon 305-700, Republic of Korea*
[b]*Display and Nanosystem Laboratory, College of Engineering, Korea University, Seongbuk-gu, Seoul 136-713, Republic of Korea*
[c]*Department of Chemical Engineering, Hanbat National University, Youseong-gu, Daejeon 305-719, Republic of Korea*

We report on the fabrication of organic thin-film transistors (OTFTs) with a reverse-offset-printed Ag metal source/drain (S/D) electrode pattern. The printed electrodes had a channel length of less than 5 μm and resistivity of 3×10^{-6} Ω cm. The OTFTs were fabricated from regioregular poly(3-hexylthiophene) as the semiconductor and poly(methyl methacrylate) as the gate insulator. The transfer and output characteristics of a top-gate OTFT with a channel length of 5 μm were evaluated. Here we discuss in detail the technological challenges encountered with reverse offset printing and the failure modes.
 [DOI: 10.1149/1.3591435]

Manuscript submitted March 17, 2011; revised manuscript received April 26, 2011. Published May 18, 2011.

Organic thin-film transistors (OTFTs) have received considerable attention because of their mechanical flexibility, low weight, and low-temperature fabrication process. With respect to device performance, there is no obstacle to real practical application of OTFTs. Organic electronic devices can be used in a wide range of applications, ranging from organic light-emitting diodes (OLEDs) for mobile phones and televisions to OTFTs for rollable displays, wearable computers, and other portable devices such as electronic paper. Other potential applications include solar-cell photovoltaics, memory, sensors, radio frequency identification cards (RFIDs), and batteries.[1,2]

Over the last several years, research has been increasingly concentrated on the development of processing methods for both functional polymers and solution-based metal electrodes for electronic devices. A great number of methods have been proposed for processing the material layers necessary for OTFT circuits, many of which are borrowed from traditional printing technologies such as offset, gravure, and flexographic printing, which are currently used primarily in the production of newspapers, books, packaging, etc. With respect to future mass production of organic electronics, a key issue is to develop ways to rely solely on these mass-printing methods for successive deposition of the different layers.[3,4]

Using printing technologies for OTFT-based applications is an exciting possibility because of the potentially high volume and low cost of production. The current state-of-the-art technology in offset and gravure printing can achieve resolutions on the order of 20 μm with a layer thickness of less than 1 μm.[3,4] However, most of the literature on the production of OTFTs is focused on inkjet or photolithographic processes.[5–7] Nevertheless, Makela et al.[8] reported an all-polymer transistor in which source/drain (S/D) electrodes are printed by using flexographic printing. Furthermore, Zielke et al.[9] fabricated OTFTs by using offset-printed S/D structures, and Huebler et al.[10] reported the first successful fabrication of an integrated circuit solely by means of fast, continuous mass-printing technology. However, the frequency of their seven-stage ring oscillator was very low (~4 Hz). The low performance of their printed organic circuit stemmed from the coarse interdigitated S/D pattern of the TFTs. Gravure-printed transistors have been demonstrated in the past, but these were typically limited to very low performance levels due to the poor line width and registration achieved in these processes.[9,10] In OTFTs, the frequency is inversely proportional to the square of the channel length.[11] Thus, the switching speed of OTFTs at high frequency will improve if the channel length L is reduced, as shown in following equation, where V_{dd} is the driving voltage and μ is the carrier mobility ($F_{MAX} = \mu V_{dd}/L^2$).

[z] E-mail: kjb0706@etri.re.kr; bkju@Korea.ac.kr

Recently, Moon et al.[12] analyzed a new direct printing method using Ag nanopowder ink for metal electrodes; this was a modified version of conventional gravure offset printing. They first coated a soft blanket roll with Ag ink and rolled it onto a glass cliché with electrode patterns. This pickup (off-step) process removes any unnecessary Ag ink outside of the electrode pattern. They then transferred the remaining Ag ink on the blanket roll to the desired glass substrate (set-step). This method is commonly called reverse offset printing. Reverse offset printing is one of mass-production printing methods that can achieve high resolution and complicate shape pattern.

In this study, we investigated the feasibility of reverse offset printing for structuring S/D areas and its applicability in the production of complete top-gate OTFTs. In addition, routes for further development were clarified by identifying the major technological challenges encountered with reverse offset printing.

Experimental

Ag electrodes with channel lengths of 5 μm or less were fabricated on glass substrates using a plate-to-plate reverse offset printer (Narae NanoTech Corporation). Ag nano paste ink (39 wt % Ag, viscosity: 1.5 cps, surface tension: 25.8 mN/m; Advanced Nano Products Co. Ltd.,) was dispensed onto the surface of the blanket roll by a syringe pump that can manipulate small amounts of Ag ink. As the blanket was rolled over the cliché with various patterns at a speed of 15 mm/s, unnecessary ink was removed from the blanket and transferred onto the top of the cliché surface. The remaining Ag ink, which was in the desired pattern on the blanket, was transferred onto 200×200 mm glass substrates in the atmosphere. The heat treatment for curing was carried out in the furnace at 450°C for 20 min in order to remove the various additives and solvent in the printed Ag ink. The resistivity of the printed Ag electrodes was calculated from the sheet resistance and thickness. Excellent fine patterns with channel lengths of 5 μm were observed by optical microscopy. Regioregular poly(3-hexylthiophene) (rr-P3HT; concentration: 20 mg/ml, regioregularity: 98%, MW = 27.3 k; Rieke Metal Inc.,) was used as the active organic semiconductor material and dissolved in *p*-xylene at 80°C for 30 min before being filtered via a 0.2 μm polytetrafluoroethylene (PTFE) syringe filter; it was then spin-coated at 2000 rpm onto the printed Ag electrodes and then cured at hotplate in N_2 atmosphere at 100°C for 30 min. The thickness of P3HT film after spinning and final curing were 60 and 50 nm, respectively. Poly(methyl methacrylate) (PMMA; MW: 120 k, dielectric constant: 3.5; Sigma–Aldrich) was used as a gate insulator. The PMMA (120 mg/ml) was dissolved in *n*-butyl acetate at 80°C for more than 2 h, spin-coated at 2000 rpm and then cured at

hotplate in N_2 atmosphere at 100°C for 30 min. The thickness of PMMA after spinning and final curing were 1350 and 1200 nm, respectively. In order to solve electrical short due to high roughness of printed Ag electrode, thick gate insulator was used. The capacitance of PMMA gate dielectric was 2.6 nF/cm^2. Finally, for the gate electrode, an Al metal film of thickness 100 nm was deposited by thermal evaporation through a metal shadow mask. The OTFT characteristics were measured by using a semiconductor parameter analyzer (4200-SCS, Keithley Instruments Inc.).

Results and Discussion

Figure 1 shows a schematic diagram of the reverse offset printing process and our device structure. Our devices consisted of four layers: the reverse-offset-printed Ag S/D electrodes, spin-coated rr-P3HT organic semiconductor, spin-coated PMMA gate dielectric, and vacuum-evaporated Al gate electrode. Figure 2 shows the line and space pattern of the reverse-offset-printed Ag electrodes. The minimum line width was 15 μm, and the minimum space between lines was 3 μm, as shown in Fig. 2. The printed minimum line width and space between lines depended on the line width and space dimensions of the cliché printing plate. These were the limit dimensions imposed by our glass cliché fabricated through a wet etching process. To prepare the cliché printing plate, Cr hard masking patterns on a glass substrate were fabricated by photolithography. The glass was then wet-etched by using an HF etchant. Line widths of less than 15 μm and line spaces of less than 3 μm could not be fabricated because of the isotropic etching property of wet etching. A cliché fabricated by dry etching or laser drilling may be needed for resolution patterns higher than those used in this study. However, there is a tradeoff between a high resolution pattern and fabrication cost of the cliché. Moon et al.[12] already reported a line width of 8 μm and space width between lines of 3 μm using reverse offset printing. Toppan[13] also reported a space width of less than 3 μm between lines using offset-based printing technology.

Figure 3 shows the transmitted optical image of an S/D electrode fabricated by reverse offset printing. As mentioned before, even though the minimum space width between lines was 3 μm, some of the patterns with 3 μm were electrically shorted by incomplete ink transfer and overflowing of Ag ink during the curing process. The channel width and length commonly used for the fabricated OTFT were 40 and 5 μm, respectively; the thickness of the electrode was 400 ± 20 nm. There was no pattern failure for S/D patterns with these dimensions. The resistivity of the Ag electrode annealed at 450°C for 20 min was 3×10^{-6} Ω cm. This is comparable to that of the AlNd or MoW electrodes commonly used in the Liquid Crystal

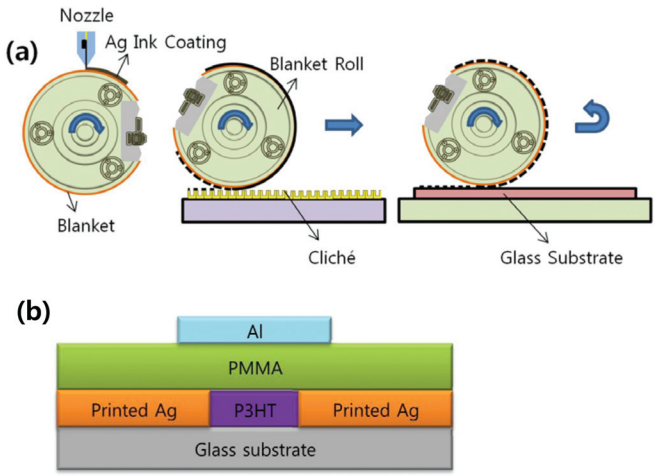

Figure 1. (Color online) Schematic diagrams of (a) reverse offset printing and (b) device structure of OTFT with the S/D electrode printed by reverse offset printing.

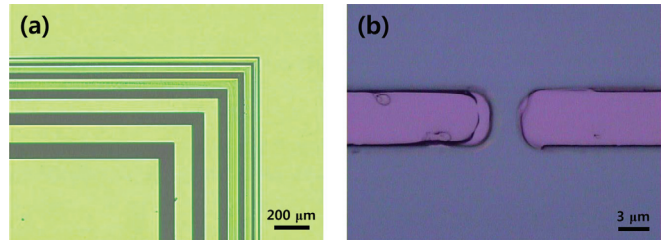

Figure 2. (Color online) (a) Various line and spacing patterns fabricated by reverse offset printing and (b) minimum spacing between lines of 3 μm.

Display (LCD) industry. High-temperature annealing conditions were chosen considering the adhesion and resistivity of Ag electrodes for S/D purposes.

The electrical characteristics of the OTFT were analyzed in the dark at atmosphere. Figure 4 shows the transfer and output characteristics of the OTFT with reverse-offset-printed S/D electrodes. The OTFT had saturation mobility (μ_{sat}) of 4.6×10^{-3} cm^2/Vs, threshold voltage (V_{th}) of −6.4 V, subthreshold swing (SS) of −24 V/decade, and on/off ratio of about 10^3.

The OTFTs with various channel width/length (W/L) of 40/20 μm, 40/10 μm, 40/5 μm, and 40/3 μm were fabricated and their characteristics were evaluated. The mobility values were 2.4×10^{-2}, 1.7×10^{-2}, 4.6×10^{-3}, and 3.0×10^{-3} cm^2/Vs, respectively. As the channel length was decreased, mobility was also decreased revealing serious contact resistance of short channel TFT. In order to compare between the conduction of deposited electrode and that of printed one, we fabricated the OTFTs with deposited Au 20 nm/Cr 3 nm electrode. The mobility of OTFT with deposited Au/Cr electrode as a reference was 1 order higher than that with reverse-offset-printed Ag electrode; μ_{sat} for deposited Au/Cr electrode was 0.12 cm^2/Vs and μ_{sat} for reverse-offset-printed Ag electrode was 0.017 cm^2/Vs. We also checked the comparison between reverse-offset-printed and evaporated Ag electrode. Surprisingly, the OTFT with reverse-offset-printed Ag electrode showed higher mobility than that with evaporated Ag one in spite of higher roughness of printed electrode.

Au is one of the conductive metals commonly used as S/D electrode for OTFT because its work function (5.1 eV for pristine Au) closely matches the highest occupied molecular orbital (HOMO) level of P3HT (4.9 eV).[14] However, the high cost of Au has been an obstacle to low-cost electronic applications. Ag electrode which has work function of 4.3 eV is energetically incompatible with P3HT.[15] The evaluated work function of our reverse-offset-printed Ag electrode by Kelvin probe method was 4.9 eV. Loo et al.[15] reported that as Ag oxidizes, its work function increases from 4.3 to

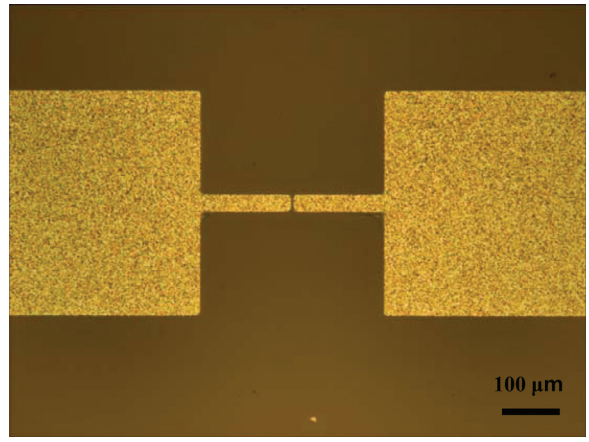

Figure 3. (Color online) S/D pattern with W/L = 40/5 μm fabricated by reverse offset printing. This pattern was used for the S/D electrode of OTFT.

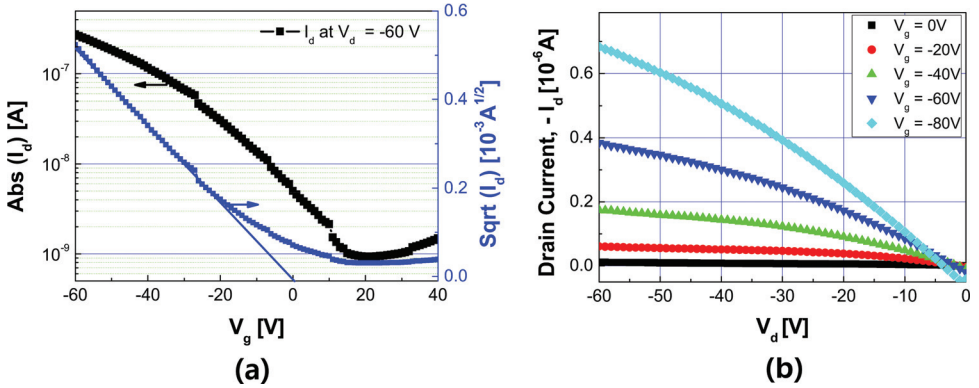

Figure 4. (Color online) (a) Transfer and (b) output characteristics of rr-P3HT OTFT with the Ag S/D electrode shown in Fig. 3.

5.0 eV and its oxidized form is conductive. Because the curing treatment of reverse-offset-printed Ag was carried out in furnace at 450°C for 20 min under low vacuum of 10^{-2} Torr, the surface of printed Ag was slightly oxidized, which was confirmed by X-ray photoelectron spectroscopy. Slight oxidation of Ag electrode increased its work function and resolved the energetic mismatch of Ag electrode with P3HT.

We believe that the reason for the relatively low performance of the short channel OTFT with the reverse-offset-printed S/D electrode—particularly, its low mobility—was the high roughness and contact resistance of Ag S/D electrode. A smooth surface on the printed areas is desirable for continuity with the subsequent layers deposited on top. This is especially the case for top-gate OTFT designs, where all other active layers have to be deposited on top of the S/D pattern. In our experiment, the root mean square roughness (R_{rms}) of the printed Ag electrode tended to increase with the grain growth. In particular, R_{rms} was less than 10 nm in the as-printed specimen and more than 80 nm for that annealed at 450°C for 20 min. In order to both fabricate Ag S/D patterns on a plastic substrate and reduce roughness, the curing temperature must be lowered. Recently, we also confirmed the effect of self-assembled monolayers (SAMs) on the contact resistance of Ag electrodes to increase device performance; this will be reported on separately.

Even though reverse offset printing is attractive due to its high throughput, high resolution, and ability to print very tiny and complicated shape patterns, it has several process problems. First, there is a high amount of waste ink, so the process cost is high. Furthermore, a roll-to-roll process is not easy due to the removal of ink on the blanket and cliché. Figure 5 shows the common failure images obtained during the reverse offset printing process. The metal Ag pattern was removed for the large pad pattern shown in Fig. 5a. We believe that the reason for this failure can be attributed to the depth of cliché pattern. If the depth of the cliché pattern is insufficient, the blanket roll can be attached to the bottom of the cliché when the blanket roll is attached onto the cliché surface; therefore, our desired Ag pattern can remain within the valley of the cliché pattern. Clichés with deep valleys are needed to prevent this type of failure. The metal Ag patterns shown in Figs. 2, 3, and 5a were fabricated using the wet etched glass cliché with the depth of 5 μm. Recently, we confirmed that the inductively coupled plasma dry etched Si cliché with the depth of 30 μm was appropriate for printing of 500×500 μm large area Ag pad pattern.

Other types of failure commonly encountered during reverse offset printing are shown in Fig. 5b. Ag electrodes are easily disconnected due to exaggerated grain growth from the high curing temperature used for reverse offset printing of Ag ink. This is another reason why we have to reduce the curing temperature of Ag ink. The Ag ink for reverse offset printing is composed of Ag nano particle, surfactant, solvent, and inorganic additive like glass frit for adhesion between glass substrate and Ag ink. Adhesion additive and glass substrate reacts at high temperature (>450°C), which gives enough adhesion properties. Organic adhesion additive such as epoxy can replace inorganic adhesion additive for low temperature annealing.

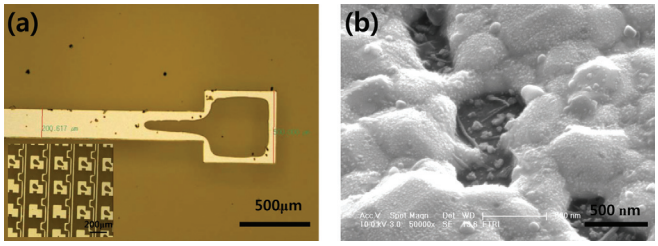

Figure 5. (Color online) (a) Common failure pattern by reverse offset printing and (b) SEM image of cured Ag electrode at 450°C for 20 min.

Conclusion

We demonstrated Ag metal electrodes patterned with line widths of 15 μm and spacing of 3 μm between lines using reverse offset printing. A resistivity of 3×10^{-6} Ω cm was obtained after thermal treatment. This is a promising result for mass-printed devices because reverse offset printing has many advantages such as high throughput and its ability to produce fine and intricate patterns. To our knowledge, this was the first trial to use reverse offset printing for the S/D electrodes of OTFT. The results show that OTFTs with acceptable characteristics can be obtained with S/D structures printed by reverse offset printing. The performance of the OTFT with 5-μm Ag S/D patterns was not satisfactory due to the high roughness and high contact resistance between rr-P3HT and the Ag S/D electrodes. Numerous printing techniques have been shown to realize simple devices or circuits. Reverse offset printing is one candidate for printing patterns, especially those that are high-resolution and complicated. This technique still has several process problems. Further study on process optimization, including ink, is needed for mass-printed devices.

Acknowledgment

This work was supported by Development of New Materials and Solution Process for LCD Backplane funded by ISTK (B551179-09-06-00), Development of Next Generation RFID Technology for Item-Level Applications (2008-F052-01) funded by the Ministry of Knowledge Economy (MKE) of Korea, and Development of Printing Ink for Touch Panel and OLED Lighting (A2010D-D006) funded by the Ministry of Knowledge Economy (MKE) and Daedeok Innopolis.

References

1. C. D. Dimitrakopoulos and P. R. L. Malenfant, *Adv. Mater.*, **14**, 99 (2002).
2. G. Horowitz, *Adv. Mater.*, **10**, 365 (1998).
3. S. R. Forrest, *Nature (London)*, **428**, 911 (2004).

4. W. Clemens, W. Fix, J. Ficker, A. Knobloch, and A. Ullmann, *J. Mater. Res.*, **19**, 1963 (2004).
5. H. Sirringhaus, T. Kawase, R. H. Friend, T. Shimoda, M. Inbasekaran, W. Wu, and E. P. Woo, *Science*, **290**, 2123 (2000).
6. S. H. Ko, H. Pan, C. P. Grigoropoulous, C. K. Luscombe, J. M. J. Frechet, and D. Poulikakos, *Nanotechnology*, **18**, 345202 (2007).
7. Y.-Y. Noh, N. Zhao, M. Caironi, and H. Sirringhaus, *Nat. Nanotechnol.*, **2**, 784 (2007).
8. T. Makela, S. Jussila, H. Kosonen, T. G. Backlund, H. G. O. Sandberg, and H. Stubb, *Synth. Met.*, **153**, 285 (2005).
9. D. Zielke, A. C. Hubler, U. Hahn, N. Brandt, M. Bartzsch, U. Fugmann, and T. Fischer, *Appl. Phys. Lett.*, **87**, 123508 (2005).
10. A. C. Huebler, F. Doetz, H. Kempa, H. E. Katz, M. Bartzsch, N. Brandt, I. Hennig, U. Fuegmann, S. Vaidyanathan, J. Granstorm, et al., *Org. Electron.*, **8**, 480 (2007).
11. A. Hoppe, D. Knipp, B. Gburek, A. Benor, M. Marinkovic, and V. Wagner, *Org. Electron.*, **11**, 626 (2010).
12. T.-H. Moon, S.-H. Nam, N.-K. Kim, Y.-K. Kook, Y.-K. Jung, Y.-G. Chang, S.-S. Yoo, C.-D. Kim, I. Kang, and I.-J. Chung, *SID Int. Symp. Digest Tech. Papers*, **40**, 1348 (2009).
13. T. Okubo, *Printed Electronics Europe*, 68, p. 1, IDTechEx, Dresden, Germany (2010).
14. J. Kim, D. Khang, J. Kim, and H. Lee, *App. Phys. Lett.*, **92**, 133307 (2008).
15. J. B. Kim, C. S. Kim, Y. S. Kim, and Y. Loo, *App. Phys. Lett.*, **95**, 183301 (2009).